Electronic Supplementary Material (ESI) for Journal of Materials Chemistry A.

Supporting information

Phase Modulation of 1T/2H $MoSe_2$ Nanoflowers for Highly Efficient Bifunctional Electrocatalysis in Rechargeable Li-O_2 Batteries

Qing Xia,[‡a] Lanling Zhao,[‡b] Deyuan Li,[a] Jun Wang,*[a,c] Lili Liu,[d] Chuanxin Hou,[e] Xiaomeng Liu,[a] Haoran Xu,[a] Feng Dang[a] and Jintao Zhang[c]

a. Key Laboratory for Liquid-Solid Structural Evolution 1and Processing of Materials (Ministry of Education), Shandong University, Jinan 250061, China

b. School of Physics, Shandong University, Jinan, 250100, P.R. China

c. Key Laboratory for Colloid and Interface Chemistry (Ministry of Education), School of Chemistry and Chemical Engineering, Shandong University, Jinan 250061, China.

d. School of Energy Science and Engineering, and Institute for Advanced Materials, Nanjing Tech University, Jiangsu Province, Nanjing 211816, China

e. School of Environmental and Material Engineering, Yantai University, No. 30 Qingquan Road, Yantai, Shandong, 264005, China

‡ These authors contributed to this work equally.

E-mail: jw707@sdu.edu.cn

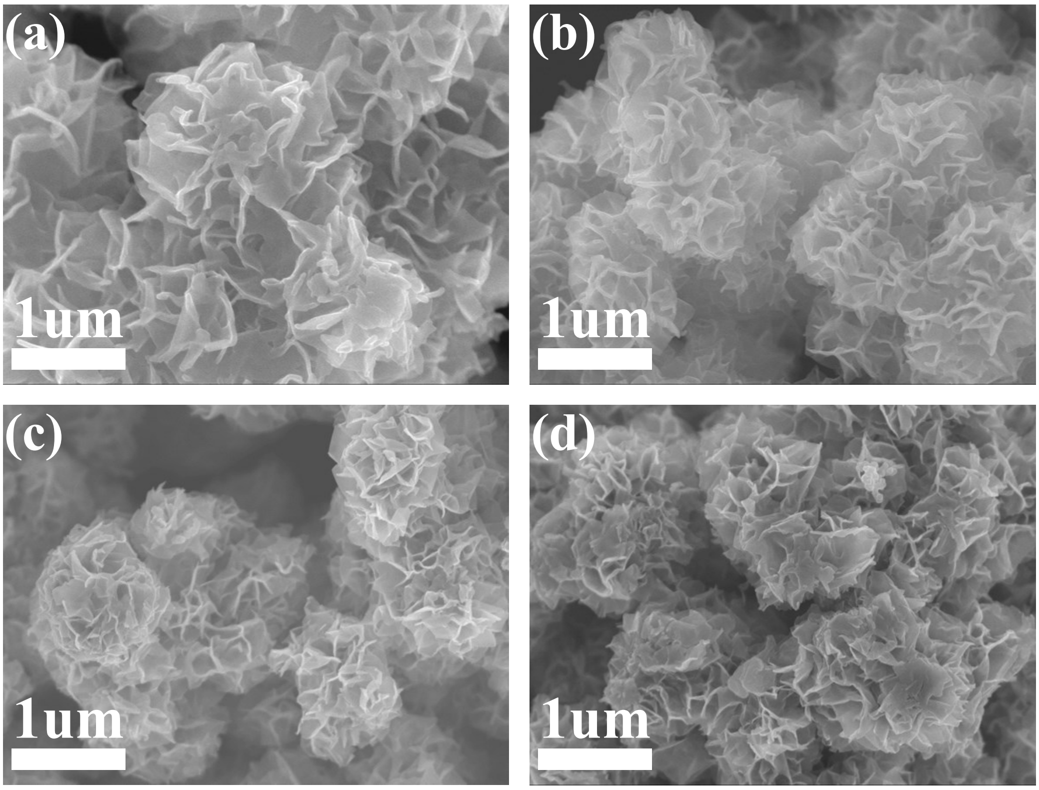

Fig. S1 SEM images of (a) MS, (b) MS-5, (c) MS-15 and (d) MS-20.

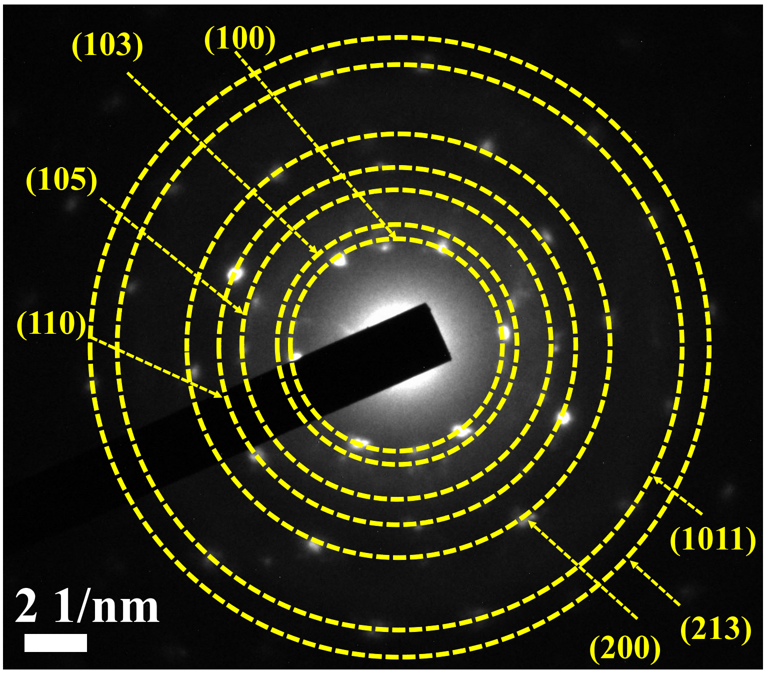

Fig. S2 SAED pattern of MS-10.

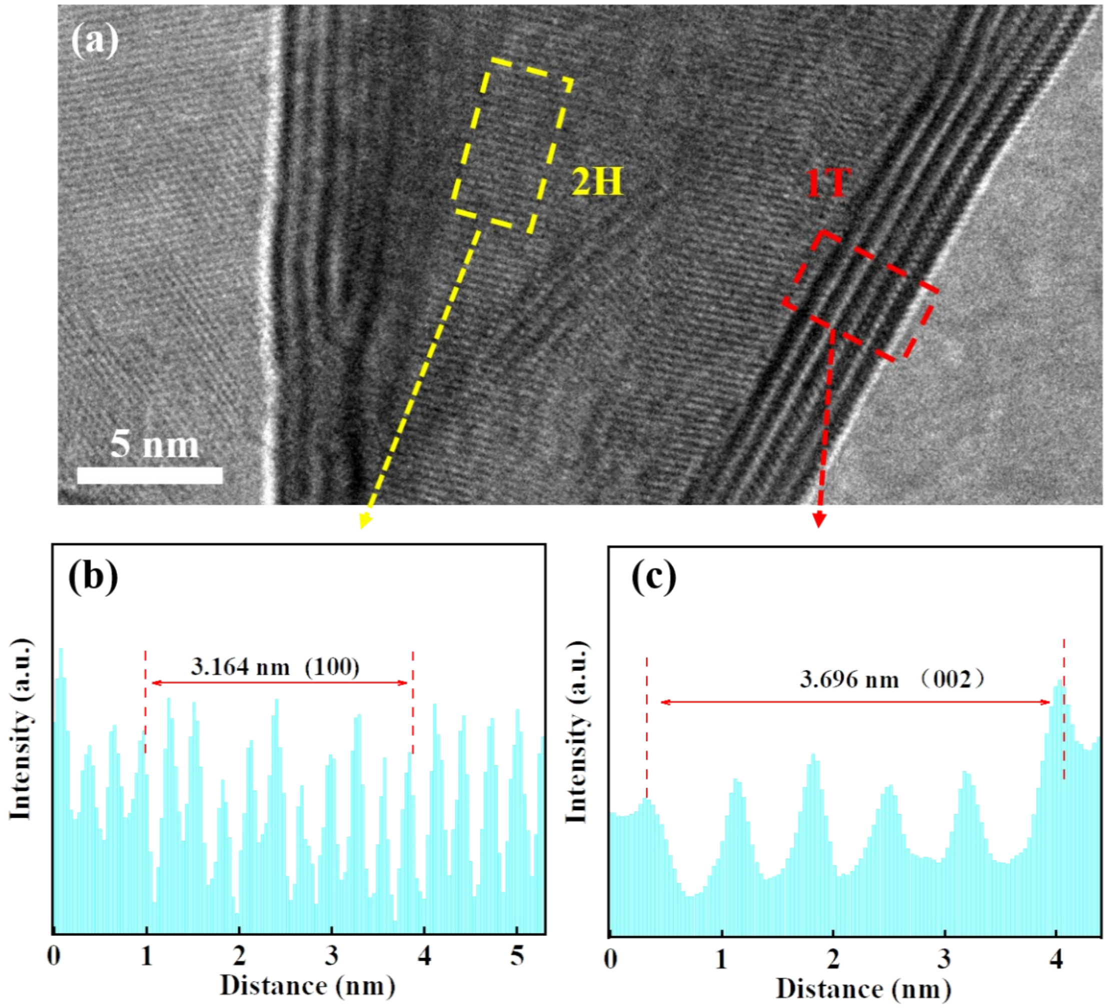

Fig. S3 (a) HRTEM image, and (b)-(c) intensity profile recorded of corresponding region of MS-10.

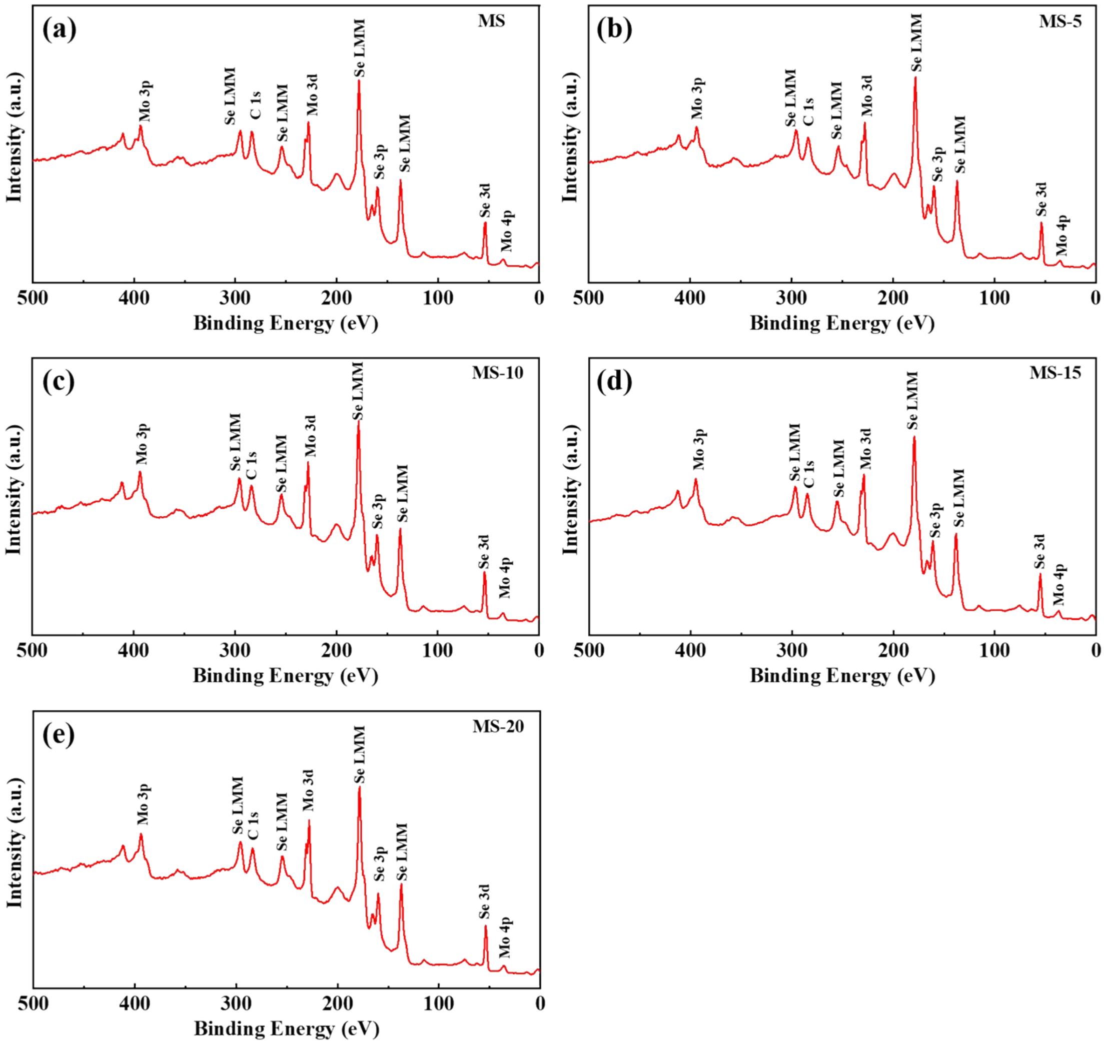

Fig. S4 Figure S4. The survey XPS spectra of (a) MS, (b) MS-5, (c) MS-10, (d) MS-15 and (e) MS-20.

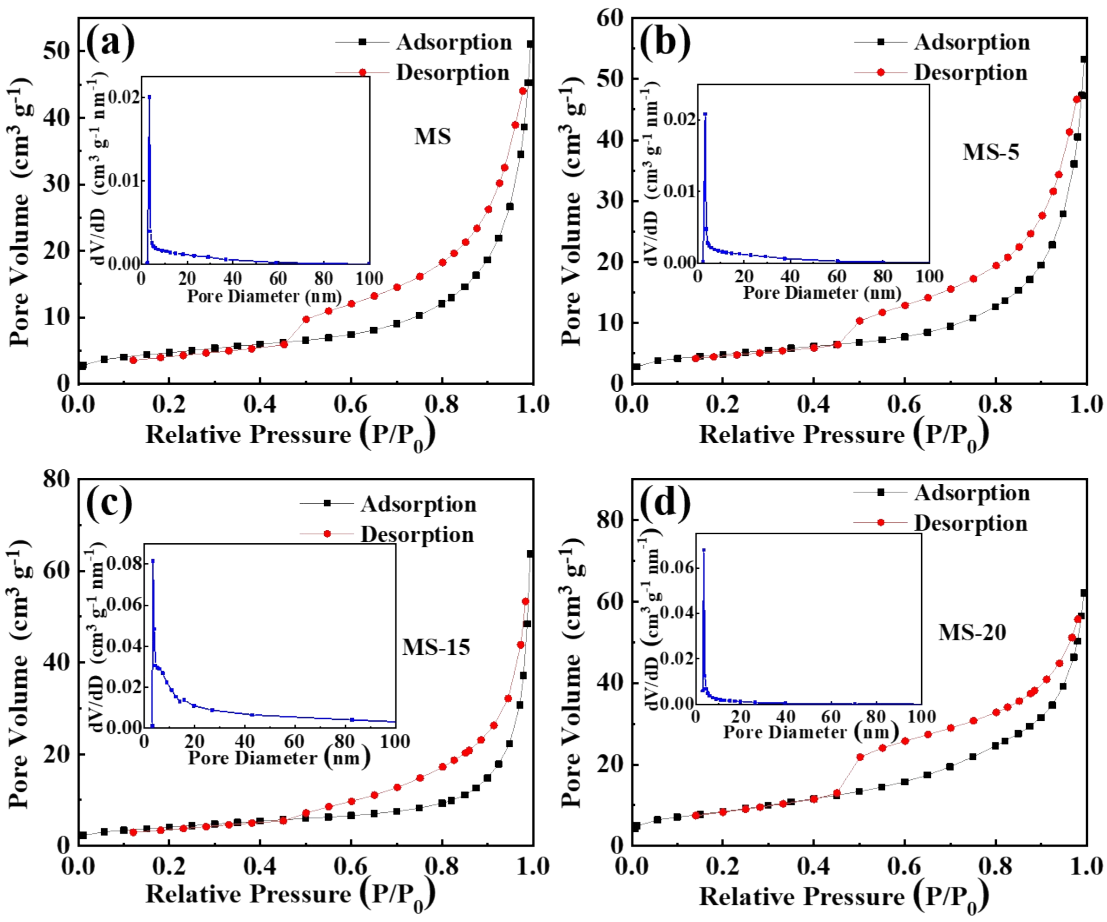

Fig. S5 The nitrogen adsorption-desorption isotherms and pore size distribution curves of (a) MS, (b) MS-5, (c) MS-15 and (d) MS-20.

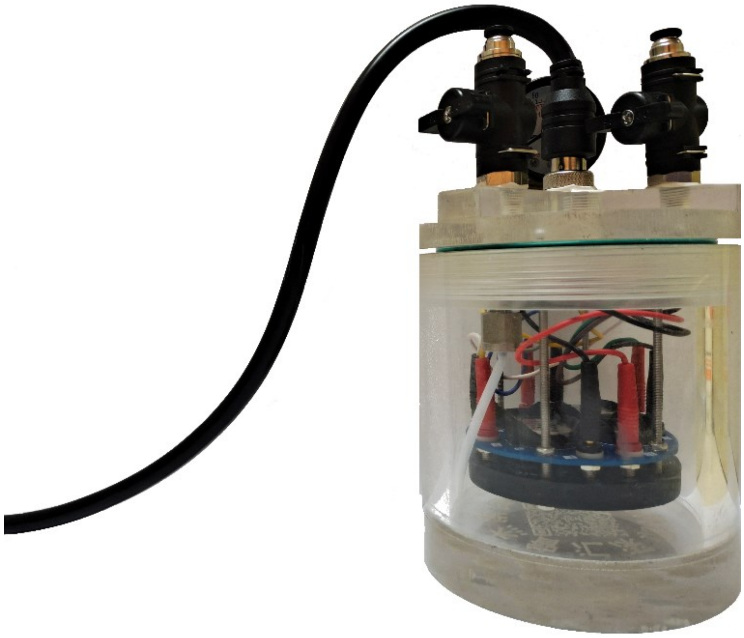

Fig. S6 The image of the hermetic container for Li-O_2 batteries purchased from NJ Scientific Ltd.

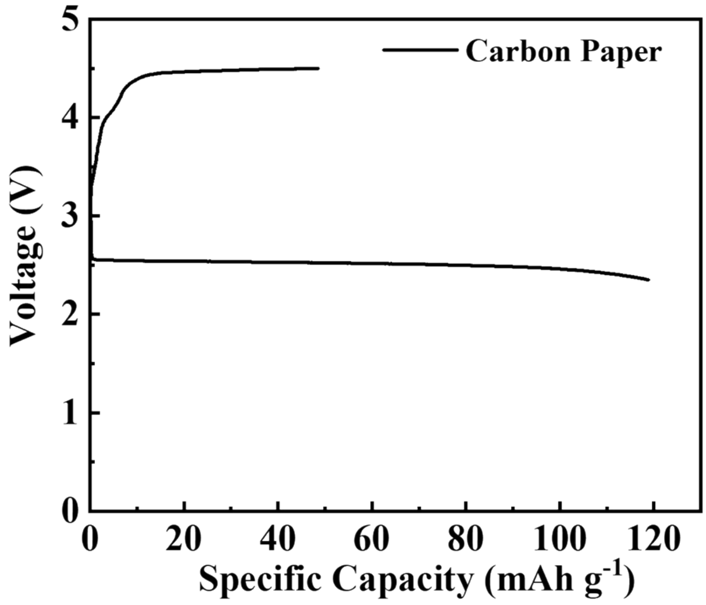

Fig. S7 Galvanostatic discharge-charge curve of pure carbon cathode at the current rate of 100 mA g^{-1}.

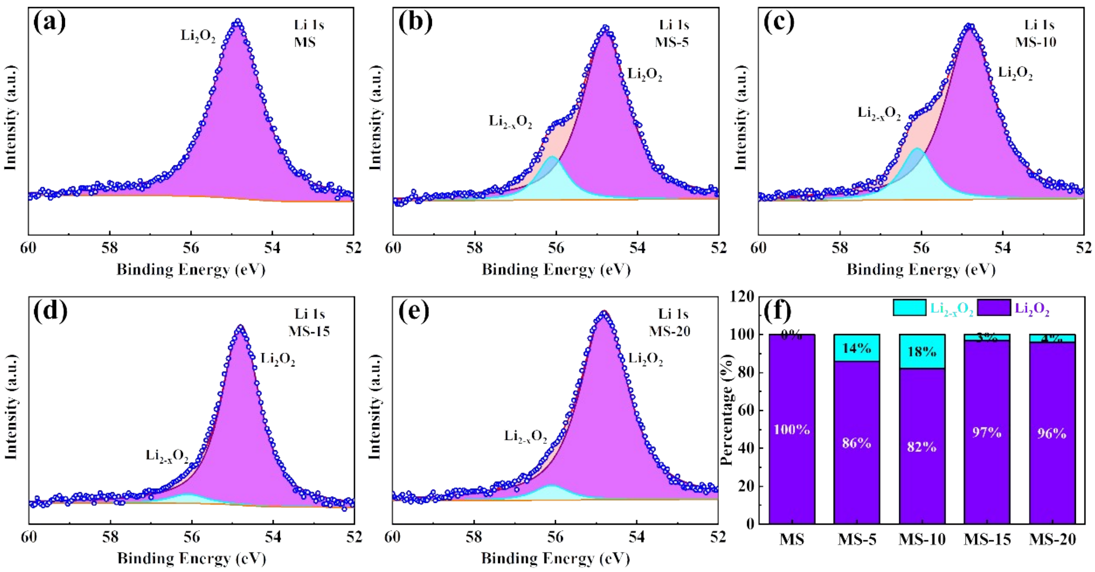

Fig. S8 (a-e) High-resolution Li 1s XPS spectra after charging to 3.5 V and (f) percentages of Li_2O_2 and $Li_{2-x}O_2$ of different cathodes.

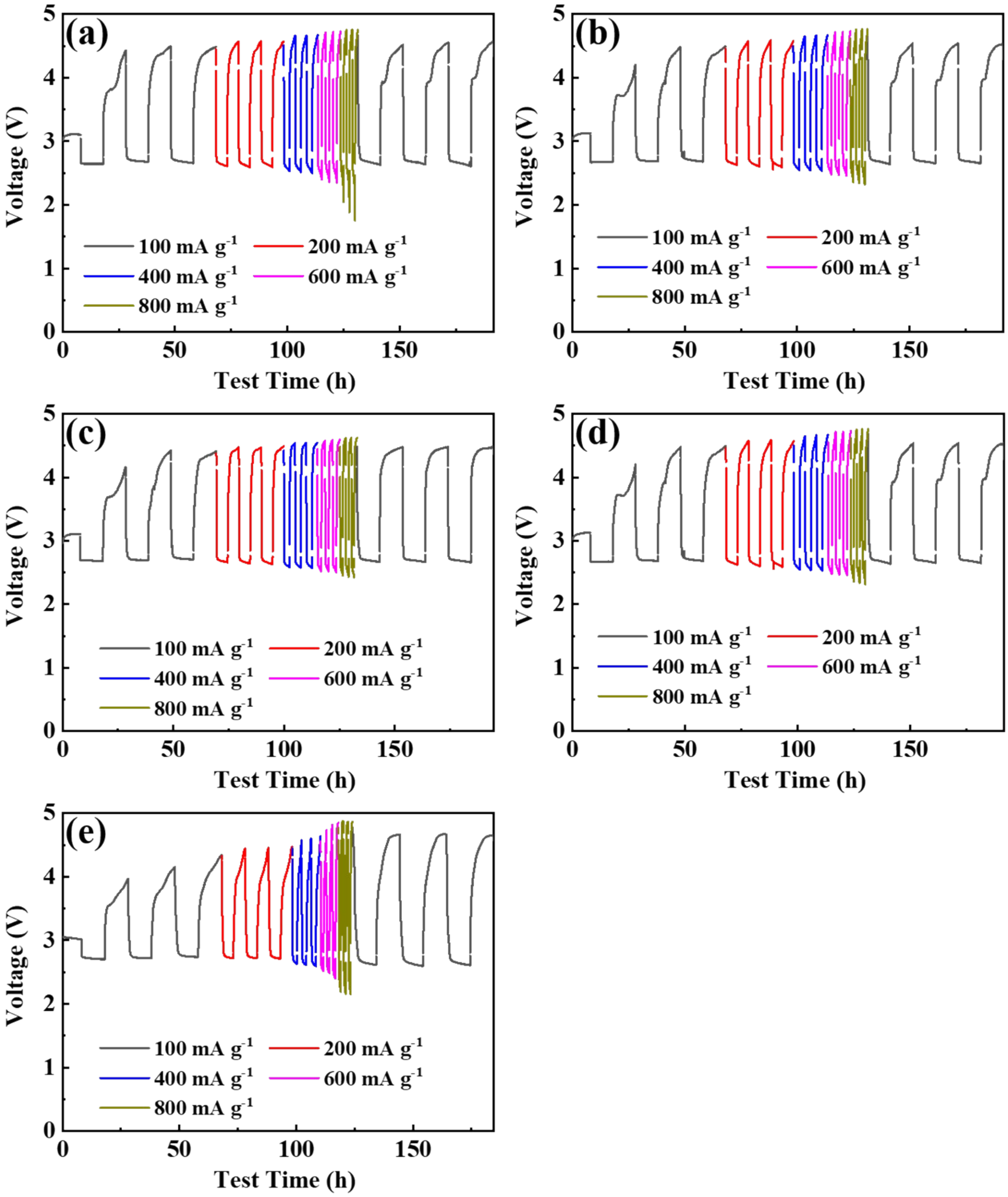

Fig. S9 Rate performance of the (a) MS, (b) MS-5, (c) MS-10 and, (d) MS-15 and (e) MS-20 cathodes.

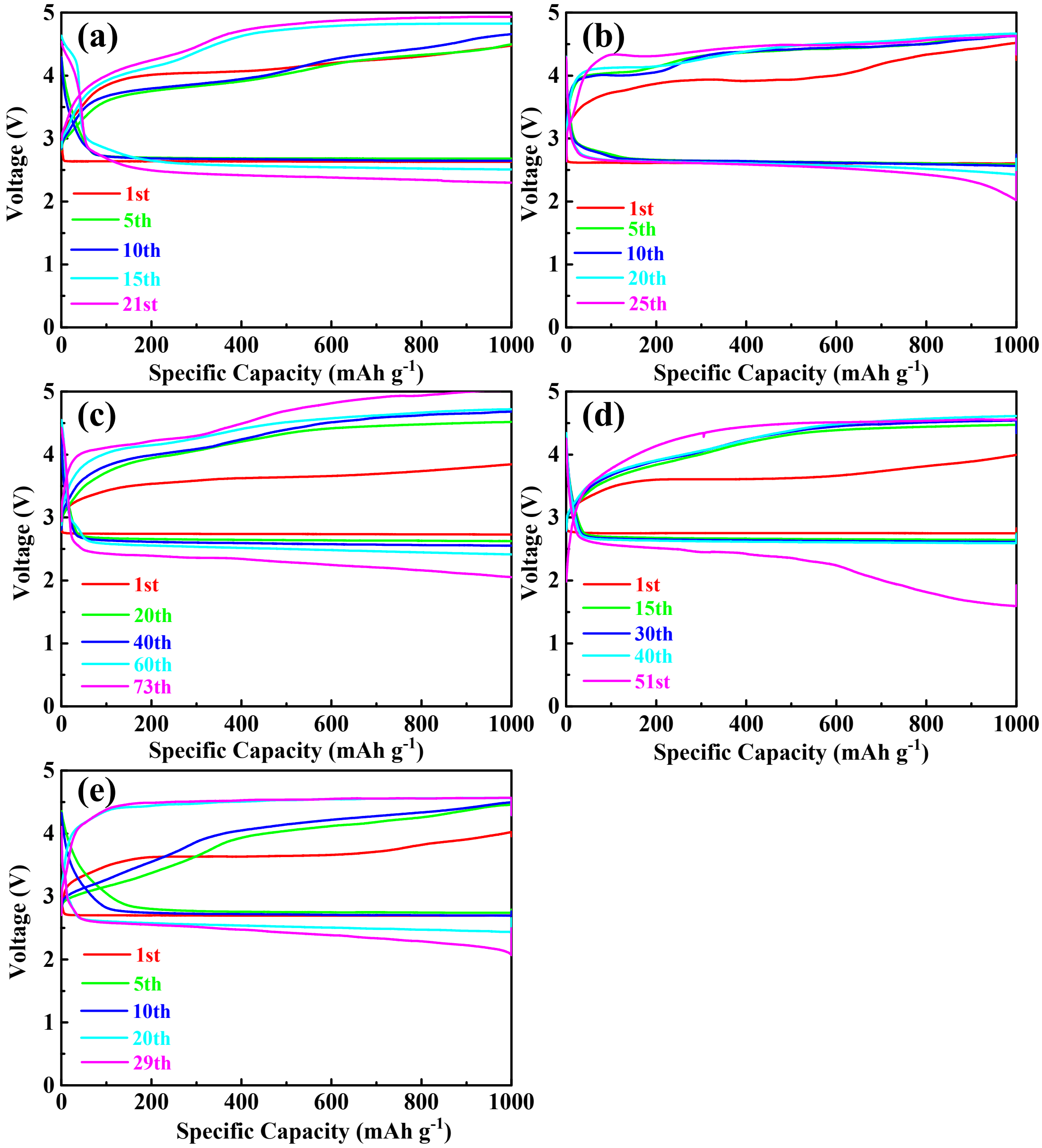

Fig. S10 Cycling performance of (a) KB, (b) MS, (c) MS-5, (d) MS-15 and (e) MS-20 cathodes at a current density of 200 mA g^{-1} with a cut-off capacity of 1000 mAh g^{-1}.

Table S1 Comparison of the Li-O_2 battery performance of 1T/2H $MoSe_2$ cathode with those of representative and most recently cathodes based on TMC catalyst reported in the literature.

Materials	1st Discharge Capacity[a]/ Current Density	Columbic Efficiencies	Cycles/Current Density-Fixed Capacity	Ref.
1T/2H $MoSe_2$ Nanoflowers	21112.4 mAh g^{-1}/ 100 mA g^{-1}	~98%	219/500 mA g^{-1}-500 mAh g^{-1}	This work
GF-CNT@MoS_2	8667 mAh g^{-1}/ 100 mA g^{-1}	~83%	190/500 mA g^{-1}-500 mAh g^{-1}-	[1]
CoS_2/CNTs	2718 mAh g^{-1}/ 0.5 mA cm^{-2}	~90%	52/0.5 mA cm^{-2}-500 mAh g^{-1}	[2]
$CuCo_2S_4$ Nanosheets	9089 mAh g^{-1}/ 100 mA g^{-1}	~97%	176/200 mA g^{-1}-500 mAh g^{-1}	[3]
1T-MoS_2/CNT	-	-	105/200 mA g^{-1}-500 mAh g^{-1}-	[4]
UC-$NiCo_2S_4$	3977 mAh g^{-1}/ 100 mA g^{-1}	~97%	144/100 mA g^{-1}-500 mAh g^{-1}	[5]
CoS_2@NC	4756 mAh g^{-1}/ 0.05 mA cm^{-2}	-	84/0.1 mA cm^{-2}-500 mAh g^{-1}	[6]
f-MoS_2/CNTs	5500 mAh g^{-1}/ 200 mA g^{-11}	~89%	140/500 mA g^{-1}-1000 mAh g^{-1}	[7]
MoS_{2-x}	8851 mAh g^{-1}/ 100 mA g^{-1}	~98%	123/500 mA g^{-1}-1000 mAh g^{-1}	[8]
Bulk MoS_2	7641 mAh g^{-1}/ 500 mA g^{-1}	-	26/500 mA g^{-1}-1000 mAh g^{-1}	[9]
MoS_2/AuNP Nanohybrids	4336 mAh g^{-1}/ 70 mA g^{-1}	~98%	50/300 mA g^{-1}-1000 mAh g^{-1}	[10]
RuO_2/MoS_2 Hybrids	4138 mAh g^{-1}/ 300 mA g^{-1}	-	45/300 mA g^{-1}-1000 mAh g^{-1}	[11]
V_{Se}-$CoSe_2$@N-CC	6089 mAh g^{-1}/ 100 mA g^{-1}	~99%	134/200 mA g^{-1}-1000 mAh g^{-1}	[12]
$FeCo_2S_4$@Ni	8724 mAh g^{-1}/ 100 mA g^{-1}	~91%	109/200 mA g^{-1}-1000 mAh g^{-1}	[13]
MoS_2/HCS	4010 mAh g^{-1}/ 100 mA g^{-1}	~93%	104/200 mA g^{-1}-1000 mAh g^{-1}	[14]
2H MoS_2 Nanosheets	6117 mAh g^{-1}/ 200 mA g^{-1}	~65%	92/200 mA g^{-1}-1000 mAh g^{-1}	[15]
2H $MoSe_2$ Nanosheets	7340 mAh g^{-1}/ 500 mA g^{-1}	~68%	86/500 mA g^{-1}-4000 mAh g^{-1}	[16]
$MoSe_2$@HCNF	4487 mAh g^{-1}/ 0.1 mA cm^{-2}	~97%	30/0.1 mA cm^{-2}-800 mAh g^{-1}	[17]

[a]The discharge capacities were calculated based on the amount of catalysts in the cathodes.

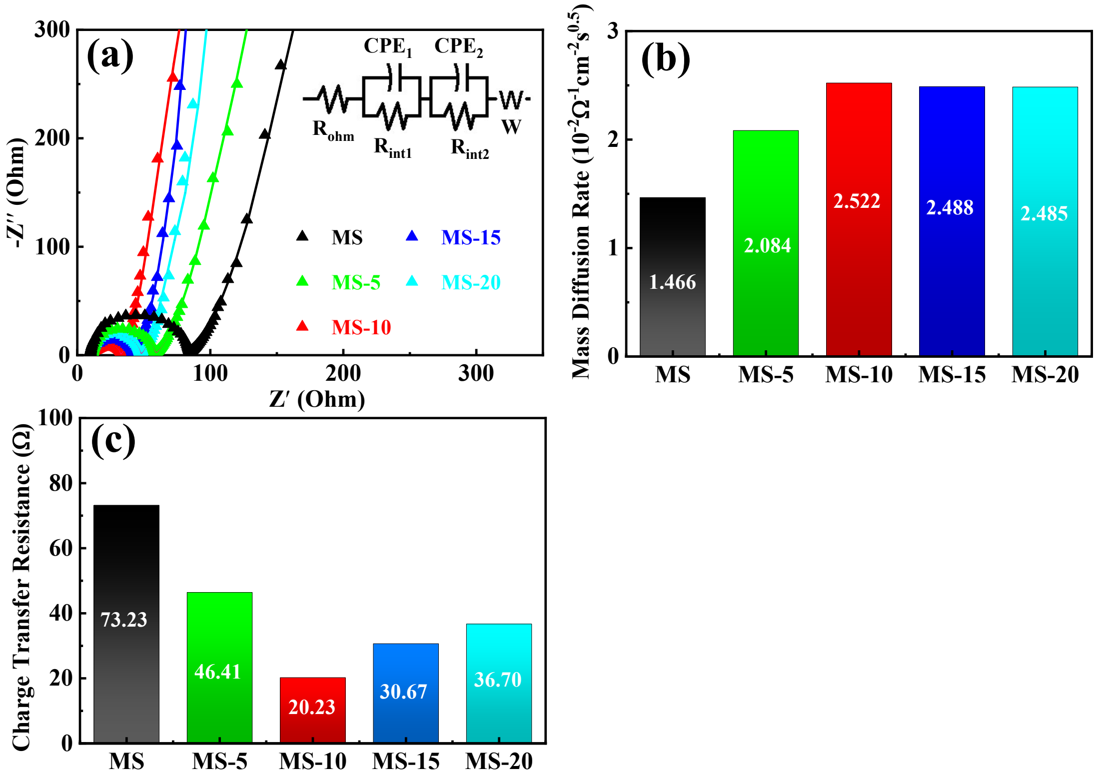

Fig. S11 (a) EIS plots at open circuit potentials with the equivalent circuit as the inset, (b) mass diffusion rates and (c) charge transfer resistances of different cathodes.

Table S2 Corresponding parameter values of the fitted EIS spectra at different states.

States	R_{ohm} (Ω)	R_{int1} (Ω)	R_{int2} (Ω)	W (10^{-2} Ω^{-1} cm^{-2} $s^{0.5}$)
Fresh	11.79	20.38	76.03	2.522
1st Discharged	12.85	80.24	173.10	0.771
1st Recharged	12.20	28.22	72.10	2.296
100th Discharged	12.02	97.20	201.63	1.577
100th Recharged	11.64	55.45	99.24	1.598

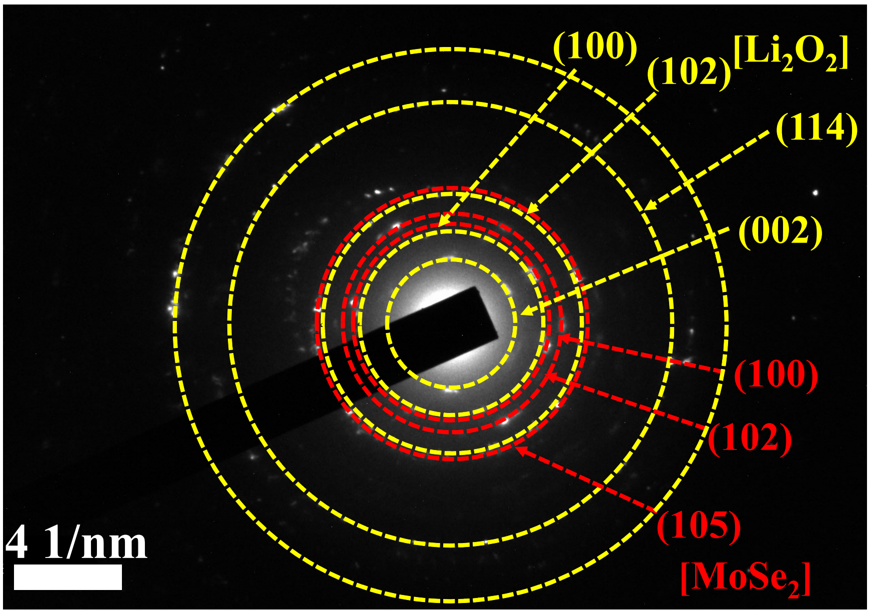

Fig. S12 SAED pattern of MS-10 cathode discharged to 800 mAh g^{-1} at 200 mA g^{-1}.

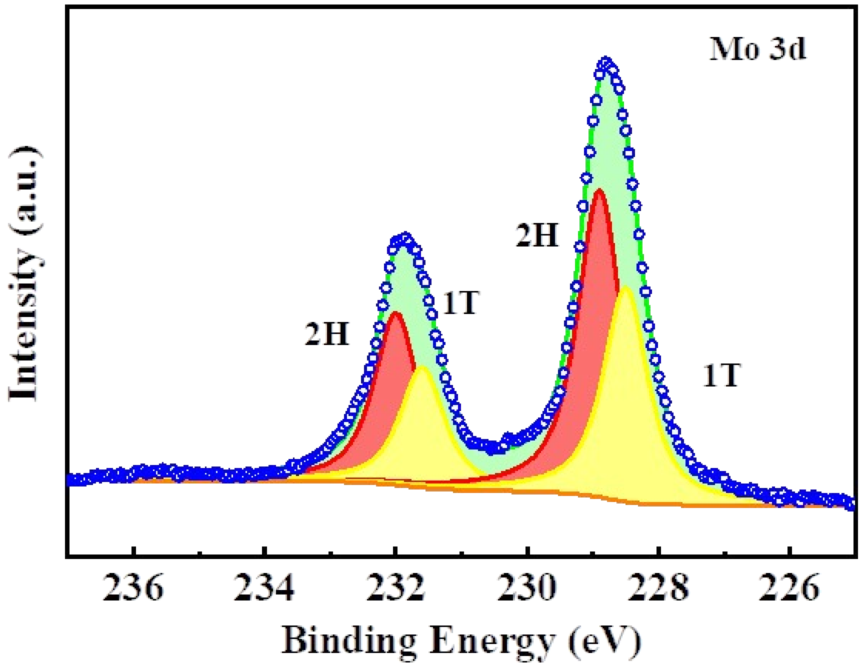

Fig. S13 High-resolution Mo 3d XPS spectrum of MS-10 cathode after cycling test.

References

1. M. Song, H. Tan, X. L. Li, A. L. Y. Tok, P. Liang, D. L. Chao and H. J. Fan, *Small Methods*, 2019, **4**, 1900274.
2. X. J. Lin, T. T. Zhang, C. C. Chu, Z. Li, R. Q. Liu, P. Li, Y. Li, Z. D. Huang and Y. W. Ma, *ACS Sustain. Chem. Eng.*, **8**, 7581-7587.
3. Z. Q. Hou, J. P. Long, C. Z. Shu, R. X. Liang, J. B. Li and X. Liao, *J. Alloys Compd.*, 2019, **798**, 560-567.
4. Z. Sadighi, J. P. Liu, L. Zhao, F. Ciucci and J. K. Kim, *Nanoscale*, 2018, **10**, 22549-22559.
5. M. T. Xu, X. Y. Hou, X. B. Yu, Z. F. Ma, J. Yang and X. X. Yuan, *J Electrochem. Soc.*, 2019, **166**, F406-F413.
6. Y. Zhan, S. Z. Yu, S. H. Luo, J. Feng and Q. Wang, *ACS Appl. Mater. Interfaces*, 2021, DOI: 10.1021/acsami.1c02564.
7. J. P. Long, A. J. Hu, C. Z. Shu, S. Wang, J. B. Li and R. X. Liang, *ChemElectroChem*, 2018, **5**, 19.
8. Y. Liu, Y. P. Zang, X. M. Liu, J. Y. Cai, Z. Lu, S. W. Niu, Z. B. Pei, T. Zhai and G. M. Wang, *Front. Energy Res.*, 2020, **8**, 109.
9. Z. M. Sun, J. L. He, M. W. Yuan, L. Lin, Z. Zhang, Z. Kang, Q. L. Liao, H. F. Li, G. B. Sun, X. J. Yang, R. Long and Y. Zhang, *Nano Energy*, 2019, **65**, 103996.
10. P. P. Zhang, X. Y. Lu, Y. Huang, J. W. Deng, L. Zhang, F. Ding, Z. Q. Su, G. Wei and O. G. Schmidt, *J. Mater. Chem. A*, 2015, **3**, 14562-14566.
11. Y. B. Jeong, Y. J. Jang, S. J. Park and Y. J. Lee, *B Korean. Chem. Soc.*, 2019, **40**, 642-649.
12. Z. Q. Hou, C. Z. Shu, R. X. Zheng, C. H. Liu, Z. Q. Ran, T. S. Yang, P. Hei, Q. Zhang and J. P. Long, *J. Mater. Chem. A*, 2020, **8**, 16636-16648.
13. Z. Hou, C. Shu, P. Hei, T. Yang, R. Zheng, Z. Ran, M. Li and J. Long, *Nanoscale*, 2020, **12**, 1864-1874.
14. A. J. Hu, C. Z. Shu, X. M. Qiu, M. L. Li, R. X. Zheng and J. P. Long, *ACS Sustain. Chem. Eng.*, 2019, **7**, 6929-6938.
15. A. Hu, J. Long, C. Shu, R. Liang and J. Li, *ACS Appl. Mater. Interfaces*, 2018, **10**, 34077-34086.
16. M. L. Li, C. Z. Shu, A. J. Hu, J. B. Li, Y. Yan, M. He and J. P. Long, *J. Alloys Compd.*, 2021, **855**, 157484.
17. Y. Q. Lai, W. Chen, Z. A. Zhang, Y. Q. Gan, X. Yang and J. Li, *RSC Adv.*, 2016, **6**, 19843-19847.